

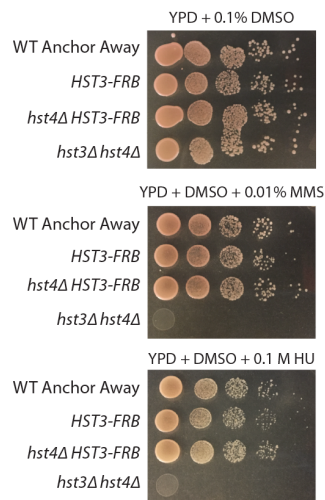
Supplemental Information

**Yeast Sirtuin Family Members Maintain
Transcription Homeostasis
to Ensure Genome Stability**

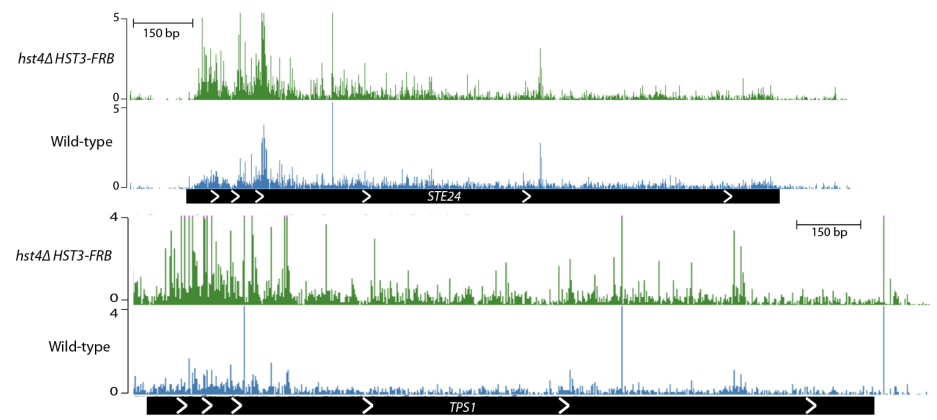
Jessica L. Feldman and Craig L. Peterson

Figure S1

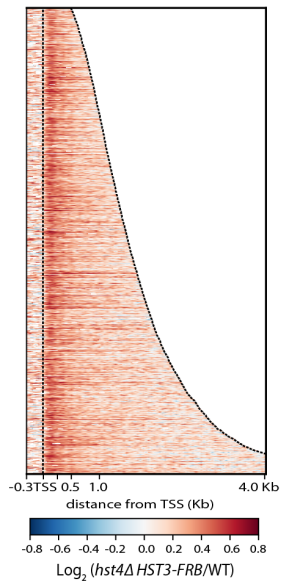
A



B



C



D

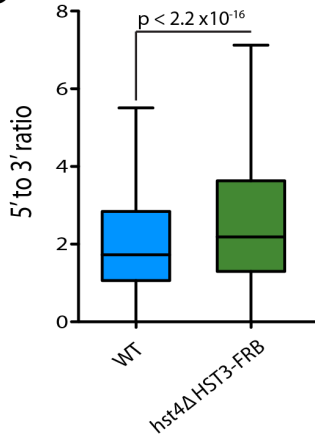


Figure S1. Hst3 and Hst4 maintain genome stability and regulate transcription, related to Figure 1. (A) WT anchor away, *HST3-FRB*, *hst4Δ HST3-FRB*, or *hst3Δ hst4Δ* strains were spotted (1/10 dilutions) on 2% glucose media containing either DMSO solvent or 8 µg/mL rapamycin (Rap), in the presence or absence of 0.01% Methyl methanesulfonate (MMS) or 0.1 M hydroxyurea (HU) and then grown for 3 days at 30°C. Note that the *hst3Δ hst4Δ* strain does not harbor the tor1-1 allele, and therefore it does not grow on rapamycin media. (B) Representative genome browser views of *S. pombe*-normalized NET-seq reads for WT (blue) and *hst4Δ HST3-FRB* (green). (C) Heatmap displaying the \log_2 fold change between *hst4Δ HST3-FRB* and WT NET-seq reads from -0.3 kb from TSS to 4 kb downstream ordered by gene length. Black dotted lines represent TSS and TTS, respectively. (D) Box plot of the 5' to 3' ratios for WT and *hst4Δ HST3-FRB* calculated by summing the reads from TSS to +250 bp divided by the sum of the reads from -250 bp from TTS to TTS. p-value determined by Mann-Whitney U-test. Four biological replicates for WT and three biological replicates for *hst4Δ HST3-FRB*.

Figure S2

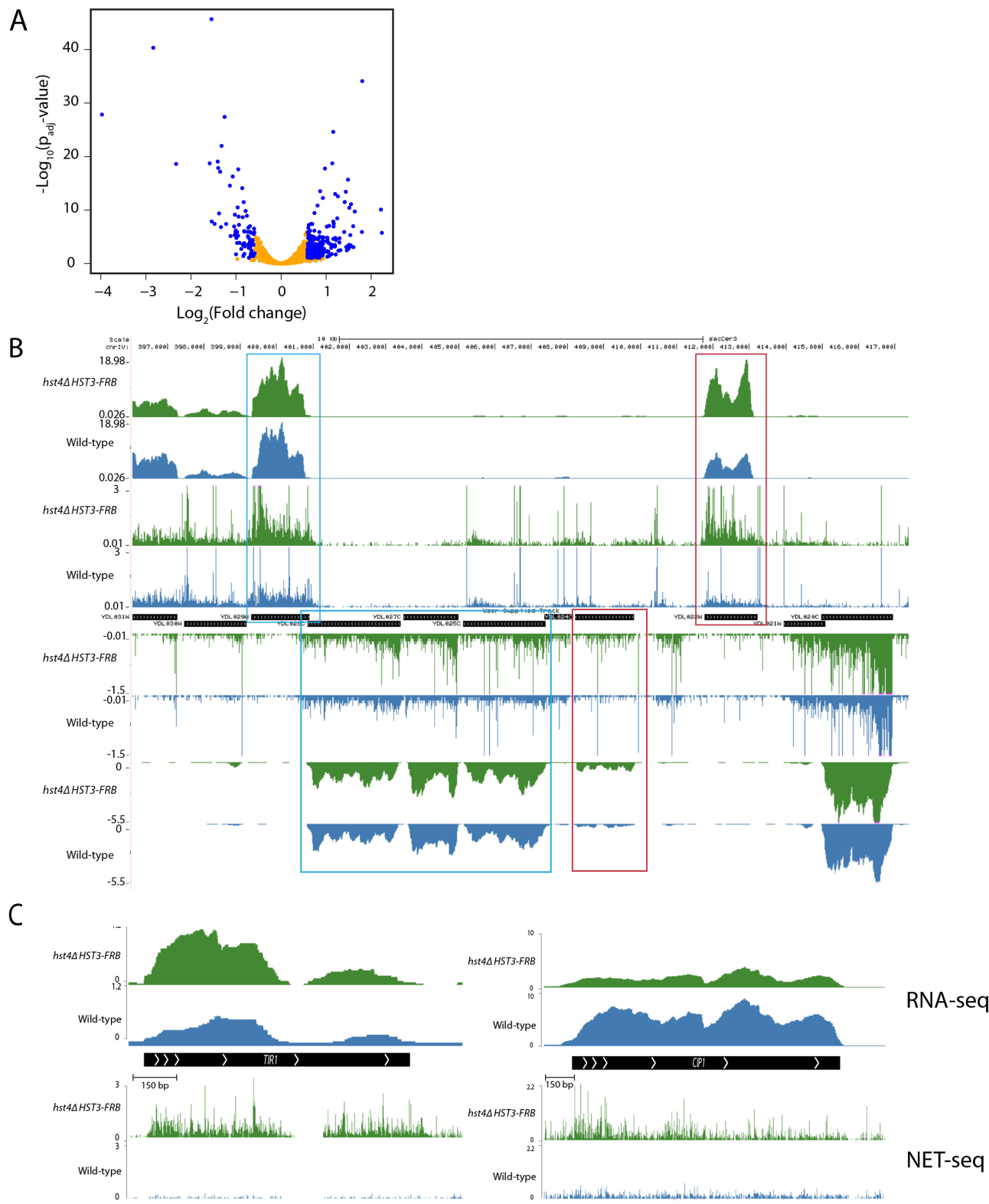
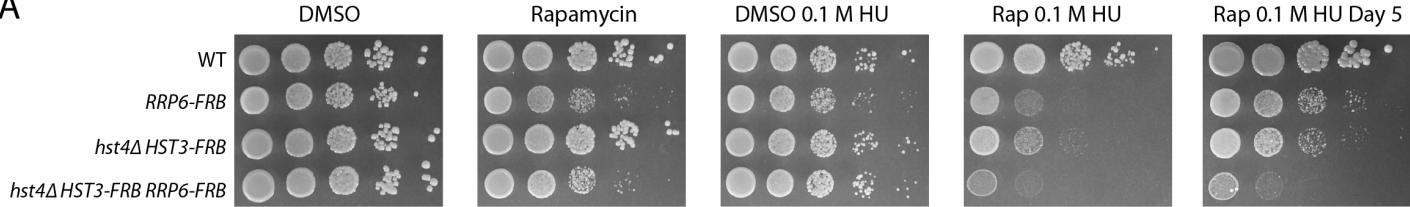


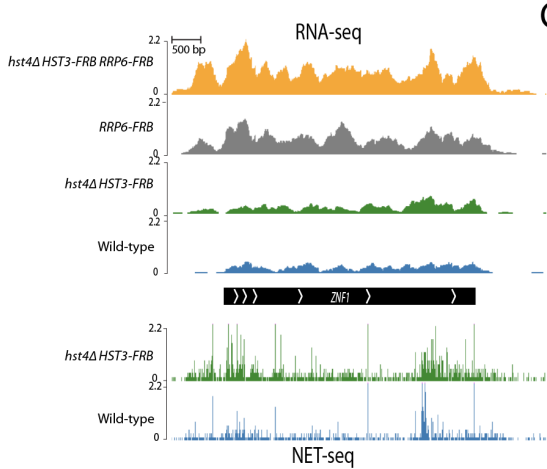
Figure S2. Steady-state mRNAs are minimally affected by loss of Hst3 and Hst4, related to Figure 3. (A) Volcano plot shows ORF transcripts that change significantly in the *hst4* Δ HST3-FRB mutant by RNA-seq. Significant genes are highlighted in blue ($p_{\text{Adj}} \leq 0.1$, \log_2 fold change ≥ 0.59 or ≤ -0.59). (B) Representative genome browser view comparing NET-seq and RNA-seq reads for WT (blue) and *hst4* Δ HST3-FRB (green). Red boxes highlight genes with increased NET-seq and RNA-seq reads in the *hst4* Δ HST3-FRB mutant. Blue boxes highlight genes with increased NET-seq reads in the *hst4* Δ HST3-FRB mutant, but not change by RNA-seq. (C) Zoomed-in genome browser view comparing NET-seq and RNA-seq reads for two representative genes for WT (blue) and *hst4* Δ HST3-FRB (green) mutants. Left, nascent and steady-state RNA increased in *hst4* Δ HST3-FRB mutant for the TIR1 gene. Right, Nascent RNA increased in *hst4* Δ HST3-FRB mutant for the CIP1 gene, but decreased steady-state RNA.

Figure S3

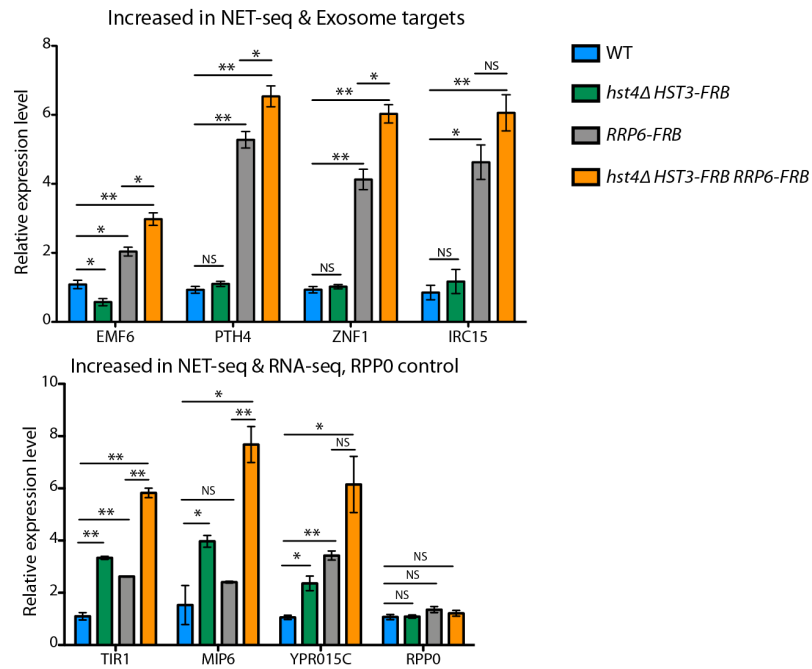
A



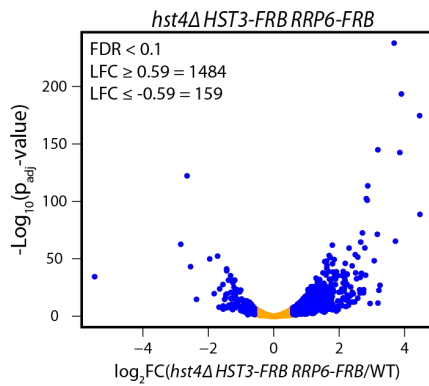
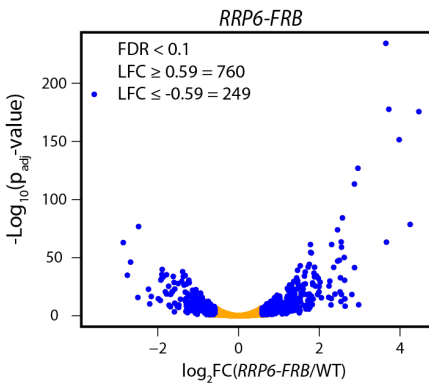
B



C



D



E

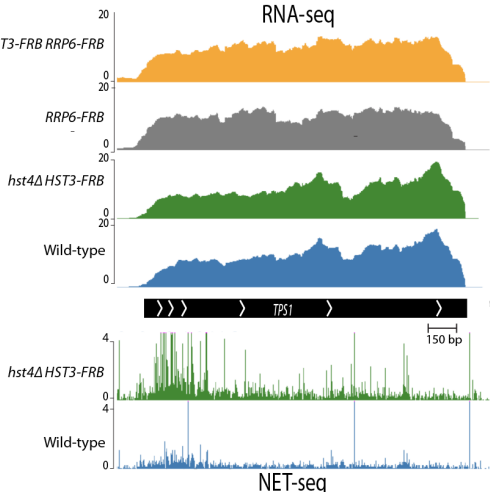


Figure S3. Nuclear exosome represses increased transcription in the *hst4Δ HST3-FRB* mutant, related to Figure 4. (A) WT anchor away, RRP6-FRB, *hst4Δ HST3-FRB*, or *hst4Δ HST3-FRB RRP6-FRB* strains were spotted (1/10 dilutions) on 2% glucose media containing either DMSO solvent or 8 µg/mL rapamycin (Rap), in the presence or absence of 0.1 M hydroxyurea (HU) and then grown for 3 days or 5 days at 30°C. (B) Genome browser view of the ZNF1 gene that is regulated by Rrp6 displaying NET-seq data (bottom) for WT (blue) and *hst4Δ HST3-FRB* (green) as well as RNA-seq data for WT (blue), *hst4Δ HST3-FRB* (green), RRP6-FRB (gray), and *hst4Δ HST3-FRB RRP6-FRB* (orange). (C) RT-qPCR confirmation of exosome targets. Left, genes with increased transcription in the *hst4Δ HST3-FRB* mutant by NET-seq, but no change or decrease in RNA-seq. Increased in the RRP-FRB mutant and further increased in *hst4Δ HST3-FRB RRP6-FRB* mutant. Right, genes increased in both NET-seq and RNA-seq in the *hst4Δ HST3-FRB* mutant and further increased in the *hst4Δ HST3-FRB RRP6-FRB* mutant. RPP0 was also included as a control gene. P-values determined by student's t-test for 2 biological replicates. (D) Volcano plot shows ORF transcripts that change significantly in the RRP6 mutant (left) or the *hst4Δ HST3-FRB RRP6-FRB* (right) by RNA-seq. Significant genes are highlighted in blue ($p_{\text{Adj}} \leq 0.1$, Log2 fold change ≥ 0.59 or ≤ -0.59). (E) Representative genome browser view of a gene that is increased by NET-seq (bottom) in the *hst4Δ HST3-FRB* (green) compared to WT (blue), but does not change in RNA-seq (top) and is not an exosome target. WT (blue), *hst4Δ HST3-FRB* (green), RRP6-FRB (gray), and *hst4Δ HST3-FRB RRP6-FRB* (orange).

Figure S4

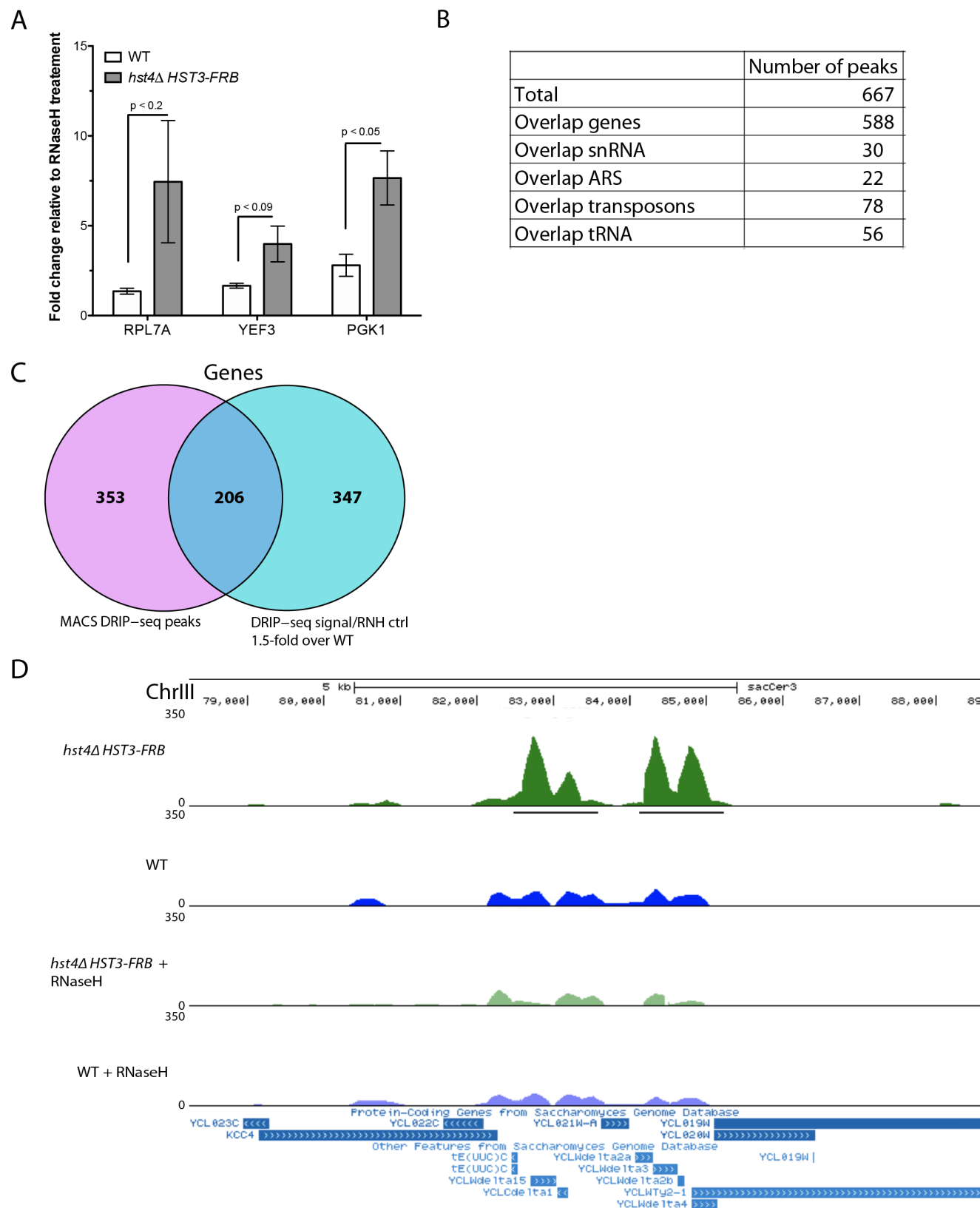
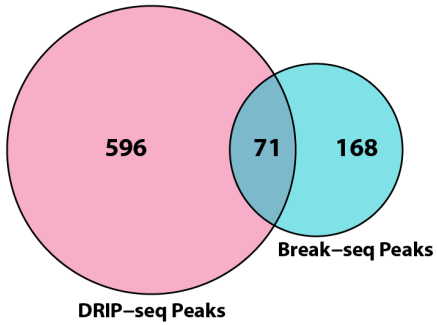


Figure S4. Increased R-loop abundance in the absence of Hst3 and Hst4, related to Figure 5. (A) DRIP-qPCR showing RNase-H normalized R-loop abundance in WT (white) and *hst4Δ* HST3-FRB (gray) for 3 biological replicates. Error bars represent standard error of the mean. P-values determined by student's t-test. (B) Distribution of DRIP-seq peaks determined by MACS for various genomic loci. (C) Venn diagram showing the overlap of DRIP-seq peaks at genes identified by MACS or by the method using an RNaseH control. (D) Representative genome browser view of normalized DRIP-seq reads in WT (blue) and *hst4Δ* HST3-FRB (green) cells at tRNA and transposon loci.

Figure S5

A



B

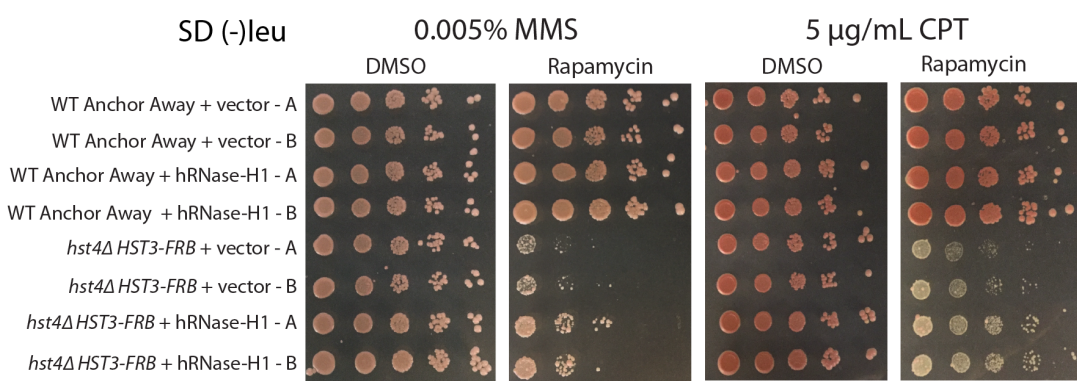


Figure S5. R-loop formation and genomic stability, related to Figure 6. (A) Venn diagram showing the overlap between Break-seq peaks and DRIP-seq peaks. (B) WT anchor away or *hst4Δ HST3-FRB* strains transformed with empty vector or a vector overexpressing human RNase-H1. Strains were spotted (1/10 dilutions) on 2% glucose media containing either DMSO solvent or 8 µg/mL rapamycin in the presence of 0.005% MMS or 5 µg/mL CPT and then grown for 3 days at 30°C. Two transformants were spotted for each strain.

Table S3.

Strains		
Name	Genotype	Source
CY1827	<i>MATa tor1-1 fpr1::loxP-LEU2-loxP RPL13A-2×FKBP12::loxP (HYH221) bar1Δ::HISG</i>	Euroscarf (Haruki et al., 2008)
CY2389	<i>MATa tor1-1 fpr1::loxP-LEU2-loxP RPL13A-2×FKBP12::loxP (HYH221) bar1Δ::HISG HST3-FRB:kanMX6</i>	This study
CY2390	<i>MATa tor1-1 fpr1::loxP-LEU2-loxP RPL13A-2×FKBP12::loxP (HYH221) bar1Δ::HISG HST3-FRB:kanMX6 hst4Δ::HPH</i>	This study
CY2028	<i>W303 MATa bar1Δ::his5+hst3Δ::NatMX hst4Δ::KanMX</i>	P. Kaufman
CY2394	<i>MATa tor1-1 fpr1::loxP-LEU2-loxP RPL13A-2×FKBP12::loxP (HYH221) bar1Δ::HISG RPB3-FLAG:NAT</i>	This study
CY2395	<i>MATa tor1-1 fpr1::loxP-LEU2-loxP RPL13A-2×FKBP12::loxP (HYH221) bar1Δ::HISG HST3-FRB:kanMX6 hst4Δ::HPH RPB3-FLAG:NAT</i>	This study
CY2474	<i>MATa tor1-1 fpr1::loxP-LEU2-loxP RPL13A-2×FKBP12::loxP (HYH221) bar1Δ::HISG RRP6-FRB:HisMX6 RPB3-FLAG:NAT</i>	This study
CY1885	<i>MATa tor1-1 fpr1::NAT RPL13A-2X FKBP12::TRP1 (HYH168)</i>	Euroscarf (Haruki et al., 2008)
CY2393	<i>MATa tor1-1 fpr1::NAT RPL13A-2X FKBP12::TRP1 (HYH168) HST3-FRB:kanMX6 hst4Δ::HPH</i>	This study
JY741/FLAG-Rpb3	h- flag-rpb3 ade6-M216 ura4-D18 leu1	NBRP (Kimura et al., 2001)
Plasmids		
Name	Description	Source
CP1458	pR5425-GPD	(Mumberg et al., 1995) From Elizabeth Tran
CP1459	pR5425-GPD-human RNase H1	(Wahba et al., 2011) From Elizabeth Tran

Table S4.

Primers		
Target	Direction	Sequence
RT-qPCR		
EMF6	Forward	5' AAGTGGTTGTGGCGGTAAAG
	Reverse	5' CCACGCACAATCCAAC TAAA
PTH4	Forward	5' AACGGGCTTGCCCTTAAATC
	Reverse	5' TCAC TTCCCTGAGGAATCCAAGC
ZNF1	Forward	5' TTGTCTAAACCCTGCTGCTACG
	Reverse	5' TCAAAGTTCCCTCGCGATGG
IRC15	Forward	5' TCGGC GGCTATTAA CATGC
	Reverse	5' CGTAA ACTGCCGCAAAATCC
OLE1	Forward	5' TTAACCGCTTCGTCATTCC
	Reverse	5' GGGGTTCTTCTGTCATCGAA
PRM7	Forward	5' AATT CCTTCACGACCAC
	Reverse	5' TCAAT GTTGCGCTGCCTTC
CIP1	Forward	5' ACCGATCCAATCCCCTTATC
	Reverse	5' AGAATT GTGCGGGCTAAGA
TIR1	Forward	5' ATT CGCTGCTATTGCTGCTT
	Reverse	5' GTCAGTGGCGGAAGCTAAAG
MIP6	Forward	5' TAGCTACGCCGATGAAACCT
	Reverse	5' GCTCGCAGATTTCCTTCTT
YPR015C	Forward	5' ACACGACCAAAAGGGAAAGTG
	Reverse	5' AAGGTGCGTAATGGTAAGCG
RPP0	Forward	5' CGGTAA CAAGGT CGGTCAAT
	Reverse	5' AGCGGAAACGAAGTGAGAAA
PDC1	Forward	5' GGTTGGGACCACCTATCCTT
	Reverse	5' TTGTGGAGCATCGAAGACTG
DRIP-qPCR		
RPL7A	Forward	5' GATCTGCC TTGTATTGTCTCG
	Reverse	5' TCAGCGGCCATTGTGATCTT
YEF3	Forward	5' GATTGCCGGTGGTAAGAAGA
	Reverse	5' CGTAAGCATCACCCATTCC
PGK1	Forward	5' GGACAAGCGTGTCTTCATCA
	Reverse	5' CGTTTCTTCACCGTTGGT